NASA
Technical Memorandum 81518

AVRADCOM
Technical Report 80-C-14

THE RESPONSE OF TURBINE ENGINE ROTORS TO INTERFERENCE RUBS

Albert F. Kascak
Propulsion Laboratory
AVRADCOM Research and Technology Laboratories
Lewis Research Center
Cleveland, Ohio

Prepared for the
1980 Army Science Conference
West Point, New York, June 17-19, 1980

NASA

THE RESPONSE OF TURBINE ENGINE ROTORS
TO INTERFERENCE RUBS

ALBERT F. KASCAK
Propulsion Laboratory
AVRADCOM Research and Technology Laboratories
Lewis Research Center
Cleveland, Ohio 44135

SUMMARY

A study was conducted to develop a method for the direct integration of a rotor dynamics system experiencing a blade loss induced rotor rub. The approach was first to insure the numerical stability of the integration technique; and second, to provide a variable time step. This was important because during the rub high frequency vibration components could be excited and smaller time steps would be necessary to calculate the vibration components accurately. During other times larger time steps could be used to conserve computational time. The method was numerically stable for any time step up to a third order integrator. The time step was controlled so that the maximum error was less then .01% and the probable error was between .001% to .0001%.

An existing rotor, (which dynamically simulates a typical small gas turbine) was modeled. The rotor bearing system consisted of a shaft with three disks mounted on two preloaded ball bearings, (two disks outboard of the bearings). The bearings were mounted in squeeze-film dampers, which had centering springs. The first three critical speeds were calculated to be 7600, 9200, and 11200 rpm; all three modes are bent-shaft type. Prior to the blade loss simulation the rotor was assumed to be balanced and operating at 9500 rpm. The blade loss was simulated by an instantaneous application of 5 mils of mass excentricity in the far disk. The rotor rub was simulated by surrounding each disk with a shroud that had a 2 mil radial clearance and a stiffness of 100,000 #/in.

In general both the blade loss and rotor rub phenomenon generate high frequency vibration components. The rotor motion is initially localized but with time progresses to other parts of the rotor by

means of traveling waves. The traveling waves from several rubs can interact with one another causing very complicated rotor motion. Even if there is no rub, (just a blade loss), the traveling wave can cause the rotor to beat at a frequency which is the difference between the operating and the critical speeds. Rotor rubs generate a frictional force which tends to drive the rotor to whirl in a direction opposite to the direction of rotation, (backward whirl). For the rotor typical of small gas turbines, a small change in the coefficient of friction, (from .1 to .2) caused the rotor to change from forward to backward whirl and to theoretically destroy itself in a few rotations. This method provides an analytical capability to study the susceptibility of rotors to rub induced backward whirl problems. A 10 minute, 16-millimeter, color, sound motion picture supplement is available, on loan, from the NASA Lewis Research Center, that shows the computer made motion pictures for the blade loss induced rotor rubs.

INTRODUCTION

In a typical aircraft gas turbine there are many instances in which rotor rubs occur. Two of the most common are blade tip and seal rubs, which are caused by thermal mismatch, rotor imbalance, high "g" maneuver loads, aerodynamic forces, etc. Current interest in fuel efficiency is a consideration which drives the engine design toward closer operating clearances. Thus increasing the probablity of rotor rubs. The interaction of a rotor with its case, (rotor rubs), has been studied in ref 1 and 2. Ref 1 studied a steady state interaction between a rotor with a rigid case neglecting friction at the interface and Ref 2 studied a steady state interaction between a linear flexible rotor and case including friction at the interface. Ref 1 and 2 did not consider the critical transient situation in which the rotor bounces off the case.

It is known that rotor rubs can have an important effect on the rotor dynamics. When a rotor rubs on the case, a frictional force is generated which can drive a rotor to whirl in a direction opposite to the direction of rotation, (backward whirl). This frictional force is relatively constant up to the backward whirl speed at which the rotor rolls around the case. Since this rolling contact speed is proportional to the rotational speed of the rotor times the ratio of the diameter to the rotor clearance, the whirl speed can be hundreds of times the rotational speed of the rotor; and thus be potentially very dangerous.

There are two basic methods for studying transient rotor dynamics. One is the modal method (ref 3 and 4) which expands the solution in terms of a few of the lower frequency mode shapes. If the transient under study is localized (like a blade loss or a rotor rub), the high frequency components are, at least initially, dominant. Thus the modal method is not applicable to this type of transient. The other method involves the direct integration of the equations of motion, which can be done in either of two ways, explicit or implicit integration. For example, ref 5 used explicit integration of the equation of motion, but this solution is plagued with numerical stability problems. Further, ref 6 showed that explicit integration of the equation of motion was unstable when the product of the critical frequency (for any mode numerically possible) and the time step was large. Therefore, the explicit integration can only be done for simple rotors.

In contrast, the implicit integration tends to be stable (ref 7 and 8) but it requires the solution of a large number of nonlinear simultaneous equations at each time step. Ref 9 used a technique similar to ref 7 except that it was applied directly to the second order equation of motion. Ref 9 also noted that the generalized forces on a rotor were functions of the generalized position and velocity of the point where the forces were applied and its nearest axial neighbors. This allowed the variables to be arranged so that the Jacobian of the set of nonlinear equations was block tridiagonal. Therefore, computing time became proportional to the number of elements in the rotor dynamics model rather than the cube of the number of elements. The objective of this study is to refine the method used in ref 9 to include an automatic time step routine and then apply the technique to study blade loss induced rotor rubs. The automatic time step routine is necessary so that the time step can be varied as the rotor impacts the case. Also, the numerical stability of the method used in ref 9 will be investigated.

SYMBOLS

- a reference amplitude
- c radial clearance
- E absolute error estimate
- F force
- O order of error in Taylor series
- q order of Taylor series
- r radial displacement
- S stability matrix
- t time
- Δt time step
- u defined in eq.(4)

z independent variable
α given set of constants
ζ damping ratio
λ eigenvalue of stability matrix
μ coefficient of friction
ω frequency

ANALYSIS

Numerical integration

Given an arbitrary vector function $\vec{z}_k(t)$ whose derivatives exist, $\vec{z}_k^{(j)}(t)$, a Taylor series expansion can be written:

$$\vec{z}_k(t + \Delta t) = \sum_{j=0}^{q-k} \frac{(\Delta t)^j}{j!} \vec{z}_k^{(j)}(t) + \vec{o}_{q-k} \qquad (1)$$

with remainder of order $\vec{o}_{q-k}$. If the arbitrary function is chosen as

$$\vec{z}_k = \frac{(\Delta t)^k}{ak!} \vec{r}^{(k)} \qquad (2)$$

the Taylor series for this function becomes

$$\vec{z}_k(t + \Delta t) = \sum_{j=0}^{q} \binom{j}{k} \vec{z}_j(t) + \vec{o}_q \qquad (3A)$$

where the binomial coefficients are defined as

$$\binom{j}{k} = \begin{cases} \dfrac{j!}{k!(j-k)!} & \text{for } j \geq k \\ 0 & \text{for } j < k \end{cases} \qquad (3B)$$

If the form of the remainder is chosen as

$$\vec{o}_q = \alpha_k \vec{u} \qquad (4)$$

the Taylor series becomes

$$\vec{z}_k(t + \Delta t) = \sum_{j=0}^{q} \binom{j}{k} \vec{z}_j(t) + \alpha_k \vec{u} \qquad (5)$$

where the alphas are given in ref 7 and $\vec{u}$ can be determined from the equations of motion at the advanced time. The form of the set of the equations of motion at the advanced time is:

$$\sum F(\vec{r}, \dot{\vec{r}}, \ddot{\vec{r}}, t + \Delta t) = 0 \qquad (6)$$

From the definition of $\vec{z}$, the various derivatives become:

$$\vec{r}^{(k)} = \frac{ak!}{(\Delta t)^k} \vec{z}_k \qquad (7)$$

Substituting for the various derivatives into the equations of motion; and knowing the values at the previous time, result in the equations of motion being a function of:

$$\sum F(\vec{u}, t + \Delta t) = 0 \qquad (8)$$

This set of equations can be solved for $\vec{u}$ and, from this value of u, the remainder can be used as an error estimate to control the time step. From the definition $\vec{z}_1$ represents a nondimensional form of $\vec{r}_1$. Therefore an estimate of the maximum absolute error is:

$$E = \alpha_1 ||\vec{u}|| \qquad (9)$$

where $||\vec{u}||$, the vector norm is the maximum component of $\vec{u}$. The computer code used in ref 9 was modified to include the following automatic time step althrogim. If E>.01%, re-do the calculation with the time step reduced by a factor of 10. If .01%>E>.001%, accept the calculation but decrease the time step by a factor of 2. If .001%>E>.0001%, accept the calculation and maintain the same time step. If .0001%>E, accept the calculation but increase the time step by a factor of 2.

Numerical stability:

The analysis of the stability of the numerical integration technique assumes a model of a rotor bearing system that is linearized at some instant of time. The homogeneous equation of motion for any mode is:

$$\ddot{r} + 2\omega\zeta\dot{r} + \omega^2 r = 0 \qquad (10)$$

where omega is the natural frequency and zeta is the damping ratio for the mode. For every mode that is numerically possible, with nonnegative damping ratio, the amplitude must either remain constant or decay in time. The numerical integration is defined as unstable if the amplitude grows in time.

Substituting the Taylor series for the various derivatives into the modal equation of motion at the advanced time results in:

$$u = -\sum_{j=0}^{q} \left[\frac{j(j-1) + 2j\omega\,\Delta t\,\zeta + (\omega\,\Delta t)^2}{2\alpha_2 + 2\alpha_1\omega\,\Delta t\,\zeta + \alpha_0(\omega\,\Delta t)^2}\right] z_j(t) \qquad (11)$$

For this value of u, the Taylor series expresses the solution at the advanced time in terms of the solution at the present time as:

$$z_k(t+\Delta t) = \sum_{j=0}^{q} \left\{ \binom{j}{k} - \frac{\alpha_k\left[j(j-1) + 2j\omega\,\Delta t\,\zeta + (\omega\,\Delta t)^2\right]}{\left[2\alpha_2 + 2\alpha_1\omega\,\Delta t\,\zeta + \alpha_0(\omega\,\Delta t)^2\right]} \right\} z_j(t) \quad (12)$$

Defining the matrix S to be:

$$s_{kj} = \binom{j}{k} - \frac{\alpha_k\left[j(j-1) + 2j\omega\,\Delta t\,\zeta + (\omega\,\Delta t)^2\right]}{\left[2\alpha_2 + 2\alpha_1\omega\,\Delta t\,\zeta + \alpha_0(\omega\,\Delta t)^2\right]} \qquad (13)$$

and the vector $\vec{z}$ whose kth element is z_k, results in the finite difference equation:

$$\vec{z}(t+\Delta t) = S\vec{z}(t) \qquad (14)$$

This equation has a solution of the form:

$$\vec{z}(t+\Delta t) = \lambda\vec{z}(t) \qquad (15)$$

where lambda is an eigenvalue of:

$$S\vec{z} = \lambda\vec{z} \qquad (16)$$

If the $|\lambda|>1$, the amplitude grows and the method is numerically unstable.

Rub model:

The interaction of a rotor with its case is a complicated phenomenon. It can involve non-linear deformation of both the rotor and the case. Rotor-case rubs were experimentally studied in ref 10. Analytically only simple rotor-case rub models are available; therefore, the case was assumed to be linear with dry friction interaction with the rotor. The radial and tangential forces on the rotor are then:

$$F_r = 0, \quad F_\theta = 0 \qquad |\vec{r}| < C \tag{17A}$$

$$F_r = -k(|\vec{r}| - C), \quad F_\theta = \mu F_r \qquad |\vec{r}| > C \tag{17B}$$

RESULTS AND DISCUSSION

The numerical method of ref 9 employed a second order integrator with a constant time step. However, to study blade loss induced rotor rubs, it is necessary to modify the method of ref 9 to include higher order integrators with an automatic time step routine. The automatic time step routine is necessary so that the time step can be varied as the rotor impacts the case. In order to calculate high frequency components accurately, the time step must be less than the period of the high frequency component. When only low frequency components are important the time step can be increased to decrease computing time. The algorithm discribed in the analysis section keeps the maximum error in the displacement at less than .01%. It tries to maintain the error between .001% to .0001% by either decreasing or increasing the time step.

Another way to decrease computing time is to use a higher order integrator. Ref 7 studied the numerical stability of up to a sixth order integrator applied to a first order differential equation. The numerical stability of these integrators applied to a second order differential equation was given in the analysis section. The numerical stability of an integrator is based on modal rotor dynamics analysis. If the integrator is applied to a mode which is not driven and has damping, the amplitude must decay in time. Figure 1 shows a stability map for the integrators used in ref 7 applied to a second order differential equation. The abscissa is the damping ratio and the ordinate is the product of the time step and natural frequency for the mode. The stability map has contours on it for which the amplitude does not change from one time to the next. On one side of the contour the amplitude grows (unstable region), and on the other side it decays. (stable region).

Figure 1 shows the stable regions for a fourth through sixth order integrator. The second and third order integrators were stable everywhere. For the regions where the integrators were unstable, the amplitude grew by a few percent per time step. It would take on the order of a hundred time steps for the amplitude to double, and it would take on the order of a thousand time steps for the amplitude to increase by a factor of a thousand. Due to round off errors, every mode that is numerically possible in the rotor dynamics model, has a finite amplitude. These amplitudes may be small but if they are in an unstable region, in a few thousand time steps they can become very large. For this reason, only the second and third order integrators were used. This is still a vast improvement over other types of integrators such as the one used by NASTRAN. NASTRAN uses an implicit form of the Newmark-Beta integrator, ref 8. This integrator is second order and does not have an error estimate.

The rotor-bearing system described in ref 11, (which dynamically simulates a typical small gas turbine), was used as the example problem. This rotor bearing system consisted of a shaft with three disks mounted on two axially preloaded ball bearings (fig 2). In this rotor-bearing system the bearings were mounted in squeeze-film damper journals, and the journals had centering springs.

The first three critical speeds for the rotor bearing system without oil in the dampers are shown in figure 3. Note that all the modes are bent- shaft modes. The "classical" hierarchy only applies to stiff shafts therefore, the classical mode shapes do not characterize the actual mode shapes. The first mode, about 7600 rpm, classically would be the cylindrical mode. But in this case, it has a large amount of bending outward near the shaft center. The second mode, about 9200 rpm, classically would be the conical mode. In this case, it has a slight amount of bending outward near the shaft ends. The third mode, about 11200 rpm, classically would be the bending mode. In this case, it has a large amount of bending throughout the shaft.

The rotor-bearing system was modeled by using 23 elements. Prior to the blade loss simulation the rotor was assumed to be balanced and operating at 9500 rpm. The blade loss was simulated by an instantaneous application of 5 mils of mass excentricity in the far disk. The equations of motion for this system were directly integrated by the method used in ref 9 with a variable time step. The output was interpolated to equal time steps (100 time steps per shaft rotation), and displayed on a CRT, figure 4. The display showed an oblique view of the rotor bearing system, with the bearing center line as the oblique axis. The transverse vibration is indicated by the position of the rotor centerline. The scale of the transverse vibration exaggerates the amplitude of the vibration. The display on the CRT was photographed at each time step. These photographs were then shown as a motion picture.

Figure 5 shows the superposition of the first ten frames of the blade loss simulation without a rub. Initially the rotor, the bearing, and the mass center line coincided. After the blade loss, a traveling wave starts at the blade loss disk and travels down the rotor. During the time high frequency components are dominant, (because the rotor as a whole is not moving). A model analysis which only uses the lower modes cannot discribe the motion during this time period.

Figure 6 shows the position of the rotor for the first six rotations of the rotor after blade loss without a rub taking place. During the first rotation, the blade loss disk spirals out. During the second rotation, the disk on the other end of the shaft spirals out. During the third rotation, the center disk spirals out. After this the envelope of the rotor positions, seems to oscillate in a conical fashion, with a frequency of about 1/4 operating speed. This beating seems to be at a frequency difference between the operating speed and the 1st critical speed. (Ref 12 experimentally showed a similiar beat frequency between the operating speed and the critical speed.) During this time the rotor shape resembles the third critical, except that the bearing center line is not in the plane of the rotor. The maximum amplitude occurred on the blade loss disk on the sixth rotation and on the opposite disk on the fourth rotation. The conclusion drawn from this figure is that if there is clearance space down the rotor and a rub occurs, it does not necessarily occur at the blade loss disk first.

The rotor-case rub was simulated by surrounding each disk with a shroud that had a 2 mil radial clearance and a stiffness of 100,000#/in. The rub was induced by a repeat of the blade loss simulation with the clearance restrain. Two rub simulations were run, one with a coefficient of friction of .1 and the other with a coefficient of friction of .2.

Figure 7 shows the first 6 rotations of the shaft after blade loss for a coefficient of friction of .1. During the first shaft rotation the blade loss disk spirals outward and bounces off the case four times. Each collision of the rotor with the case sends out traveling waves down the rotor. These waves interact with each other causing the envelope of the rotor motion to be very complicated. On the second shaft rotation both outboard disks bounce off the case four times. As the rotor continues to turn the orbit becomes more circular. That is, the rotor-case interaction becomes less of a bouncing nature and more of a continuous contact. The envelope of the rotor motion seems to be oscillating in a conical nature; but both outboard disks seem to remain in contact with the case. The rotor continues to whirl about the bearing centerline in the rotational direction (forward whirl). The frictional drag forces are not large enough to drive the rotor into backward whirl.

Figure 8 shows the first 4 rotations of the shaft after blade loss for a coefficient of friction of .2. The motion of the rotor on the first rotation is similar to the .1 coefficient of friction case. On the second rotation, the blade loss disk has a very hard collision with the wall, causing the rotor to bend considerably. On the third rotation the rotor whirl direction changes from forward to backward whirl and the rotor whirl begins to accelerate in the backward direction. On the fourth rotation, the rotor motion becomes very large and it continues to grow on succeeding rotations.

This example problem has shown that small changes in the coefficient of friction, (from .1 to .2) can change a rotor response to a blade loss condition from a relatively safe response to a catastrophic response. For seal rubs the coefficient of friction is probably between .1 to .2. For blade tip rubs, this rub model is not accurate. This type of rub involves material removal, phase changes, and or non-elastic deformations. If this model were to be used in a general manner, then the coefficient of friction would probably be greater then .2.

In conclusion, this computer code allows us to look at blade loss induced rotor rubs and displays the rotor motion in a motion-picture format. A 10-minute, 16-millimeter, color, sound motion-picture supplement is available, on loan, that shows the computer made motion picture for the blade loss induced rotor rubs.

SUMMARY OF RESULTS AND CONCLUSIONS

A method for direct integration of a rotor dynamics system experiencing a blade loss induced rotor rub was developed. The following conclusions were drawn:

1. The method was numerically stable for any time step up to a third order integrator.

2. The time step was controlled so that the maximum error was less then .01% and the probable error was between .001% to .0001%.
3. For the rotor typical of small gas turbines a small change in the coefficient of friction, (from .1 to .2), caused the rotor to change from forward to backward whirl and to destroy itself in a few rotations.
This method provides an analytical capability to study the susceptibility of rotors to rub induced backward whirl problems.

REFERENCES

1. Johnson, D.C.: Synchronous Whirl Of A Vertical Shaft Having Clearance In One Bearing. J. Mech. Eng. Sci. vol.4, No.1, 1962, pp 85-93.
2. Black, H.F.: Interaction Of A Whirling Rotor With A Vibrating Stator Accross A Clearance. J. Mech. Eng. vol.10, No.1, 1968, pp 1-12.
3. Childs, D.W.: A Rotor-Fixed Model Simulation Model Of Flexible Rotating Equipment. J. Eng. ind., Vol.96, No.2, May 1974, pp 659-669.
4. Gunter, E.J. et al.: Transient And Stability Analysis Using The Modal Method. UVA/528144/ME77/102, University of Virginia, 1977.
5. Shen, F.A.: Flexible Rotor Dynamics Analysis. (R-9252, Rocketdyne: NASA Contract NAS3-14422.) NASA CR-121276, 1973.
6. Kascak, A.F.: Stability Of Numerical Integration Techniques For Transient Rotor Dynamics. NASA TP-1092, 1977.
7. Gear, C.W.: The Automatic Integration Of Stiff Ordinary Differential Equations. Proc. IFIP Congress Information Processing 68 (Edinburgh 1968), A.J.H. Morrell ed., Vol.1, Mathematics Software, North Holland Publ. Co., Amsterdam 1969, pp 187-193.
8. Newmark, N.M.: A Method Of Computation For Structural Dynamics. J. of the Eng. Mech. Div., Proc. of the American Soc. of Civil Eng. Paper No.2094, Vol.85, No. EM3, July 1959, pp 67-94
9. Kascak, A.F.: Direct Integration Of Transient Rotor Dynamics. NASA TP 1597, AVRADCOM TR 79-42, Jan 1980.
10. Bill, R.C. and Wisander, D.W.: Friction And Wear Of Several Compressor Gas-Path Seal Materials. NASA TP 1128, 1978.
11. Cunningham, R.E.; Fleming, D.P.; and Gunter, E.J.: Design Of A Squeeze-Film Damper For A Multi-Mass Flexible Rotor. ASME Trans. J. Eng. Ind., Vol.97, No.4, Nov. 1975, pp 1383-1389.

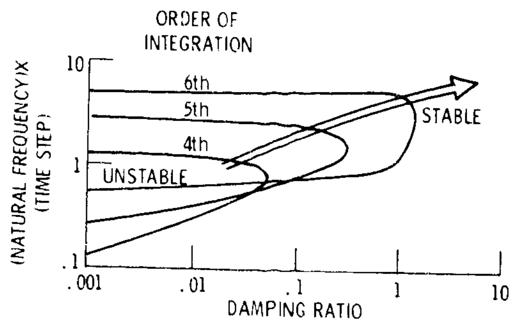

Figure 1. - Numerical stability of Gear's integration method applied to a second order differential equation for a 2nd thru 6th order of integration. The 2nd and 3rd order methods are always stable.

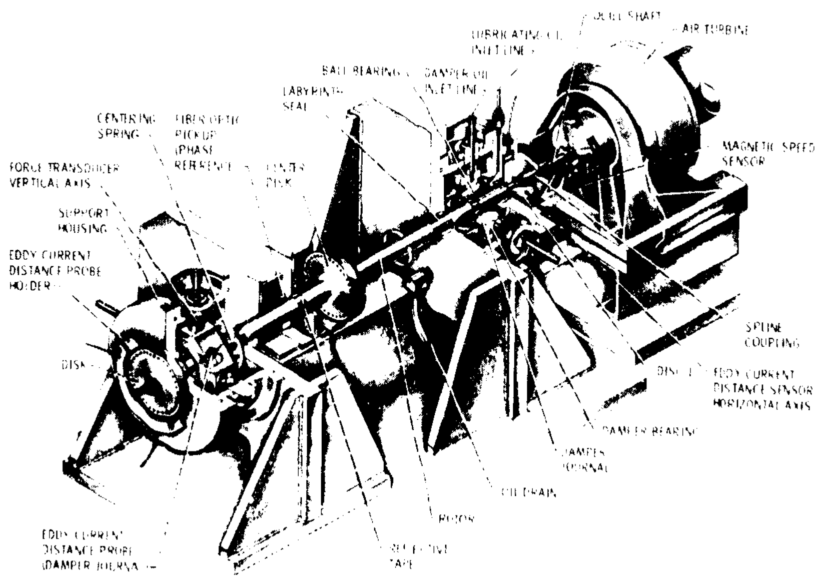

Figure 2. - Schematic of test apparatus used in experiments on steady-state unbalance response.

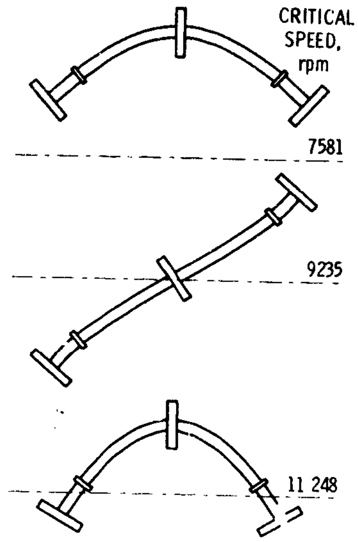

Figure 3. - Critical speeds and mode shapes.

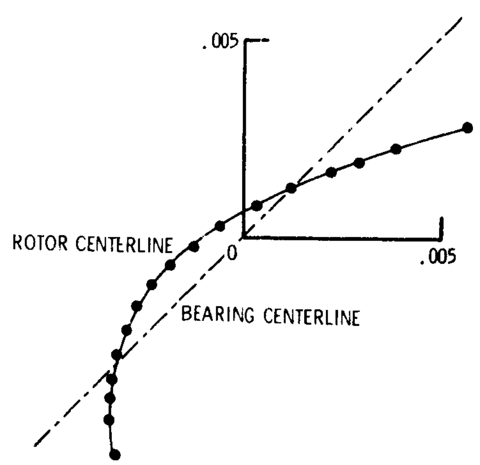

Figure 4. - Oblique view of rotor centerline whirling about the bearing centerline.

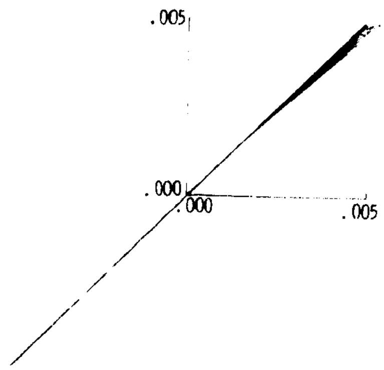

Figure 5. - Initial movement of rotor after blade loss.

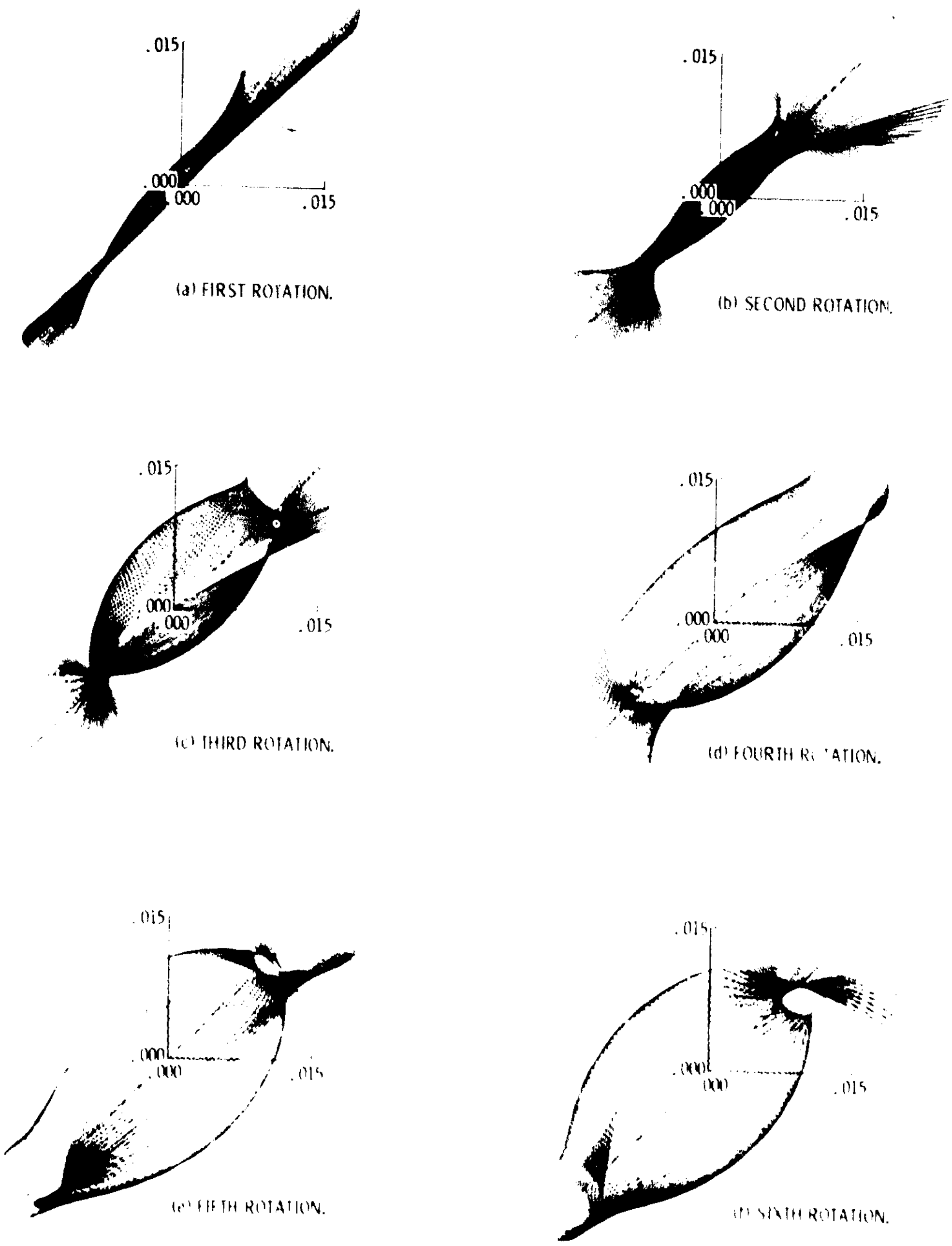

Figure 6. Envelope of rotor motion for first six rotations of rotor after blade loss (without a rub taking place).

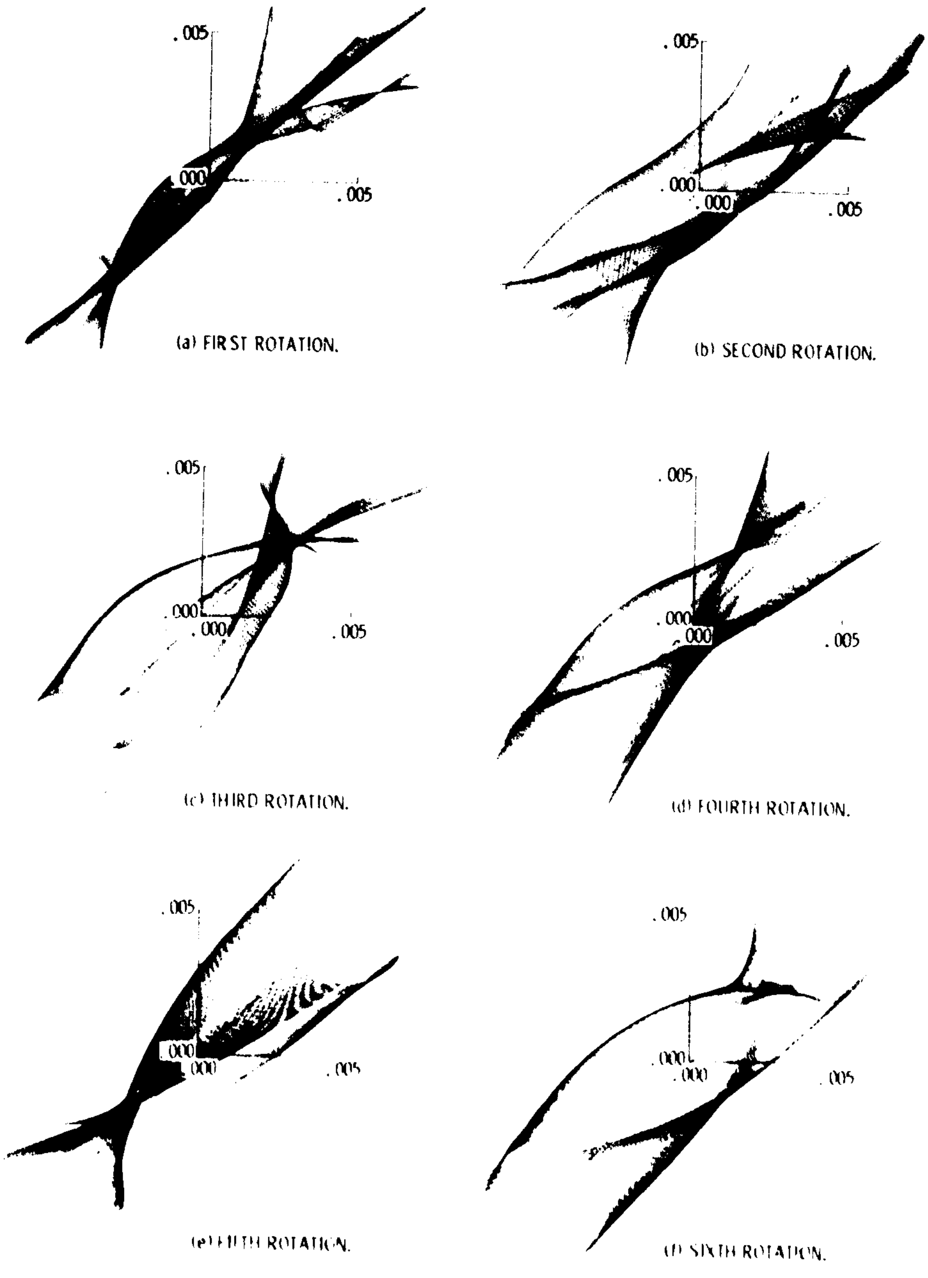

Figure 7. Envelope of rotor motion for first six rotations of rotor after blade loss (coefficient of friction equals 0.1).

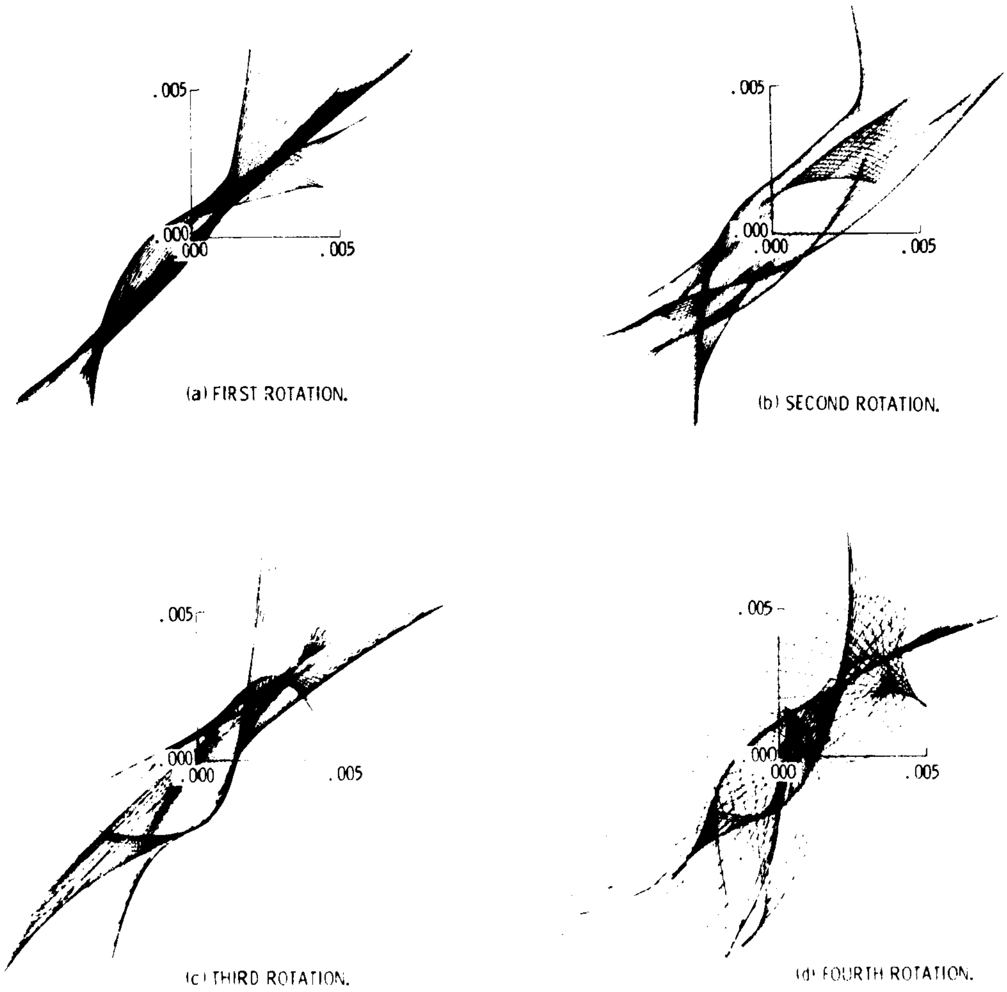

Figure 8. - Envelope of rotor motion for first four rotations of rotor after blade loss (coefficient of friction equals 0.2).

END

DATE

FILMED

SEP 8 1980